Measure The Built Environment for Children Via Google Street View (GSV) Data: A Case Study in Villach, Austria

The Marshall Plan Scholarships

Austrian Marshall Plan Foundation

Final Research Paper

Yutian Zeng

Department of Geography and Anthropology

Louisiana State University

Supervisor Host Institution

Dr. Gernot Paulus

Department of Geoinformation and Environmental Technologies

Carinthia University of Applied Science

Supervisor Home Institution

Dr. Michael Leitner

Department of Geography and Anthropology

Louisiana State University

Contents

List of Figures

List of Tables

Abstract

Childhood obesity is a critical health challenge globally, particularly in Europe. However, limited research has focused on the association between child health and the built environment. Traditional methods for measuring environmental factors often rely on subjective, self-reported data, underscoring the need for more objective, standardized approaches. This study addresses this gap by utilizing Google Street View (GSV) data to objectively measure and analyze environmental variables that impact children's health in Villach, Austria. GSV offers eye-level imagery, providing a practical, accessible approach for capturing urban and suburban environments. This research quantifies green spaces, constructions, transport infrastructure, and sky view ratios, comparing the urban center and suburban tech park to reveal substantial differences in environmental factors. Spatial analysis using Moran's I further examines spatial patterns of these variables, assessing how resource distribution may shape children's health behaviors.

1   Introduction

According to the World Health Organization (WHO), obesity has been considered one of the major health challenges facing countries in the European Region regions (Breda et al., 2021). Obesity is related to other negative health conditions like high blood pressure, high cholesterol, type 2 diabetes, breathing problems and others(Stierman et al., 2021). Childhood obesity and overweight are a particularly pressing and serious challenge, as early health status and exposure influence disease risk later in life (Ortegon-Sanchez et al., 2021).

Environments are important factors of consideration for childhood obesity prevention and control (Malacarne et al., 2022). Due to their rapid growth and unique physiological development, children are more sensitive to the impact of environmental exposures (World Health Organization, n.d.). Their systems, including immature central nervous, immune, reproductive, and digestive

5

systems, can suffer irreversible damage from exposure to toxicants during developmental stages(Gascon et al., 2016; World Health Organization, n.d.). Furthermore, unlike adults, children lack the autonomy, awareness, and decision-making capacity to safeguard their health through their behavior (Ding et al., 2011; World Health Organization, n.d.). However, Smith et al. (2017) found that there is a lack of research regarding children, whereas the adults-centered approaches may not adequately capture the context that is important to children. Despite their importance, the association between child health and the built environment has received comparatively less attention than in adult populations (Barrett et al., 2017).

It has been demonstrated that there is a strong connection between the urban physical environment and various health behaviors. Recent research has increasingly focused on the connection between obesogenic environments and childhood obesity. Nevertheless, current studies lack standardized methods for measuring food environments but relying on self-reported data that emphasize subjective perceptions (Kang et al., 2020). In this context, Google Street View (GSV) data presents an effective alternative for studying environmental measurements due to its cost-effectiveness, time-efficiency, and widespread accessibility. GSV images data can provide eye-level imagery even in some less developed areas, making it a valuable source of big data for various research.

This study aims to measure and analyze environmental factors influencing children's health in Villach, Austria, using GSV data. The research questions guiding this study are as follows:

1) Measurement via GSV data: How to measure the environment variables via GSV data? Can GSV data and machine learning measure the built environment accurately?

2) Spatial disparities in Villach: What are the spatial differences in the built environment between urban and suburban areas in Villach?

3) Spatial pattern in Villach: What is the spatial pattern of the health-related environment in Villach?

The significance of this study lies in its contribution to the understanding of how environmental factors can be quantitatively assessed using GSV data, offering a more nuanced perspective compared to traditional methods. Additionally, it highlights the importance of considering both urban and suburban contexts when evaluating the impact of the built environment on children's health.

Section 2 discusses the literature concerning the health environment and application of GSV data. Section 3 presents the workflow of the methodology including the data, model, and spatial analysis method. Section 4 covers the model selection, discusses the comparison between urban and suburban areas, as well as the environment and the spatial environmental pattern in Villach. Section 5 concludes this study and discusses its limitations and future research directions.

2   Literature Review

The literature review synthesizes findings from two critical areas of research: the environmental factors influencing childhood obesity and the application of Google Street View (GSV) data in assessing these environments. The first section explores how various community characteristics affect children's health behaviors and outcomes. The second section will discuss the utility of GSV data in providing a nuanced understanding of the built environment, emphasizing its role in capturing detailed features that influence physical activity and overall health.

2.1   Environment and health behavior

A number of societal and community factors affect children's obesity and children that are overweight. These include child care and school environments; neighborhood design; access to

healthy, affordable food and beverages; and access to safe and convenient places for physical activity (PA), which collectively affect our ability to make healthy choices (CDC, 2022). A recent review by Ortegon-Sanchez et al. (2021) summarized ten types of built-up, environmental factors: Residential or population density, intersection density (street connectivity), land-use diversity, walkability, street-level walking infrastructure, perceptions of street environments, accessibility to recreation and sports facilities, proximity to school as a determinant for active travel, access to public open spaces, safety perceptions, motorized traffic levels, and social support and psychosocial factors. These factors may facilitate or inhibit physical activity and diet intake behaviors, which may in turn continuously impact residents' energy balance. The study areas are normally around children's home, school, or their route to/from school (Ortegon-Sanchez et al., 2021).

Natural elements like green and blue spaces, which encompass vegetation (e.g., trees, grass, forests, and parks) and visible water bodies, have been a focal point of health behavior research. The presence of street greenery has been proved to link to higher odds of walking, which is an important aspect of physical activity that contributes to overall health (Lu et al., 2018). Additionally, access to green spaces has been shown to positively influence travel satisfaction, well-being, and mental health, highlighting the significant impact of the built environment on individual health outcomes (Ta et al., 2021; Wang et al., 2019).

Durand et al. (2012) expanded the understanding of children's physical activity to include active transport. Active transport like walking and bicycle improved the fitness levels of physical activities(PA), though it tended to be overlooked in some related research (Smith et al., 2017). Longitudinal studies by Carver et al. (2011) revealed moderate correlations between children's physical activity and active transport at ages 5-6 and 10-12, indicating that active commuting

during childhood can foster long-term health benefits. Active transport for children's commuting behavior may encounter various restrictions, such as the distance between school and home, or an environment that lacks pedestrian- and cyclist-friendly infrastructure (Carver et al., 2011). In the review of the effect of the built environment on active transport and PA, Smith et al. (2017) summarized a positive impact on active transport and PA through walkability features, provision of quality parks and playgrounds, and installation of or improvements in active transport infrastructure.

2.2   The application of GSV data

GSV data provided street-level images that can more intuitively reflect the actual human perception of the surrounding environment(Li et al., 2015; Zhang et al., 2023). Through the comparison between virtual data from GSV and in-person survey , Clarke et al.(2010) found that virtual audit instruments can indicate recreational facilities, the local food environment, and general land use. Compared to traditional methods such as surveys and interviews commonly used in related research, Google Street View (GSV) data offers an avenue for objective measurement (Feuillet et al., 2016). It has been proved that GSV data outperform traditional secondary data in capturing fine-grained features, such as sidewalks and obstructions, providing more accurate and detailed insights (Kang et al., 2020). For instance, Ben-Joseph et al. (2013) highlighted its effectiveness in capturing details like sidewalks and obstructions. Larkin and Hystad (2019) found the street view based green space measurement has less correlation with other measurements using remote sensing images, which suggests that street view images capture unique information. Despite important limitations, GSV has been recognized as a "promising tool for automated environmental assessment for health research"(Rzotkiewicz et al., 2018).

From the perspective of GSV applications, Rzotkiewicz et al.(2018) identified health behaviors and outcomes as major themes, encompassing physical activity (walking or biking),

mental health, health-related behaviors (smoking, alcohol consumption), and injuries (traffic crashes, disasters). In the review of street view imagery in public health studies, Kang et al.(2020) classified the application of street view images into element representation and scene representation. Element-level representation involves observing individual objects within street view images (e.g., trees, water bodies, traffic lights), while scene representation captured the entire scene and understood the context, such as the land-use type, environmental equality, and personal perception including safety and environmental aesthetics (Kang et al., 2020).

A common element-based metric is the Green View Index (GVI), which quantifies visible green space by calculating the proportion of green pixels within an image. Li et al. (2015) enhanced the GVI method by expanding from four to six images to capture a full 360-degree horizontal view and introduced three vertical angles per sampling point. This modification aims to more accurately replicate the pedestrian viewpoint in environmental assessments. Making the measurement more comprehensive. Zhang et al. (2023) measured the GVI based on the panorama view images. Similarly, Sky View Factor (SVF), which represents the ratio of visible sky to the total view area in an image with the range from 0 to 1, was also utilized to measure the environment (Xia et al., 2021). Wang and Vermeulen (2021) employed a comparable method, categorizing elements including vegetation, pedestrian infrastructure, and sky to assess the built environment, allowing for a simplified yet informative view of environmental factors relevant to physical and mental well-being.

This study employs an element-based approach, categorizing environmental features into green space, construction, transport infrastructure, and sky view. Green space and construction are seen as contrasting elements; generally, an abundance of green space is associated with increased physical activity and improved mental health for children. The sky view serves not only as a

contextual background but also as an indicator of open environments. Transport infrastructure is indicative of commuting convenience and walkability; while higher levels may facilitate accessibility, they can also imply potential traffic hazards. The measurement process involves segmenting each image into these categories and calculating the area of each segment as a proportion of the total image area.

3   Methodology

This study aims to assess the urban and suburban environments of Villach, Austria, using Google Street View (GSV) data, specifically to select the appropriate models and measure the environment in these areas, and the environment surrounding primary schools. Section 3.1 briefly introduces the coverage of Google Street View (GSV) data. Section 3.2 introduces the Deeplabv3 model trained on different datasets and how to choose a pre-trained model for image segmentation. Section 3.2 discusses further analysis after image segmentation.
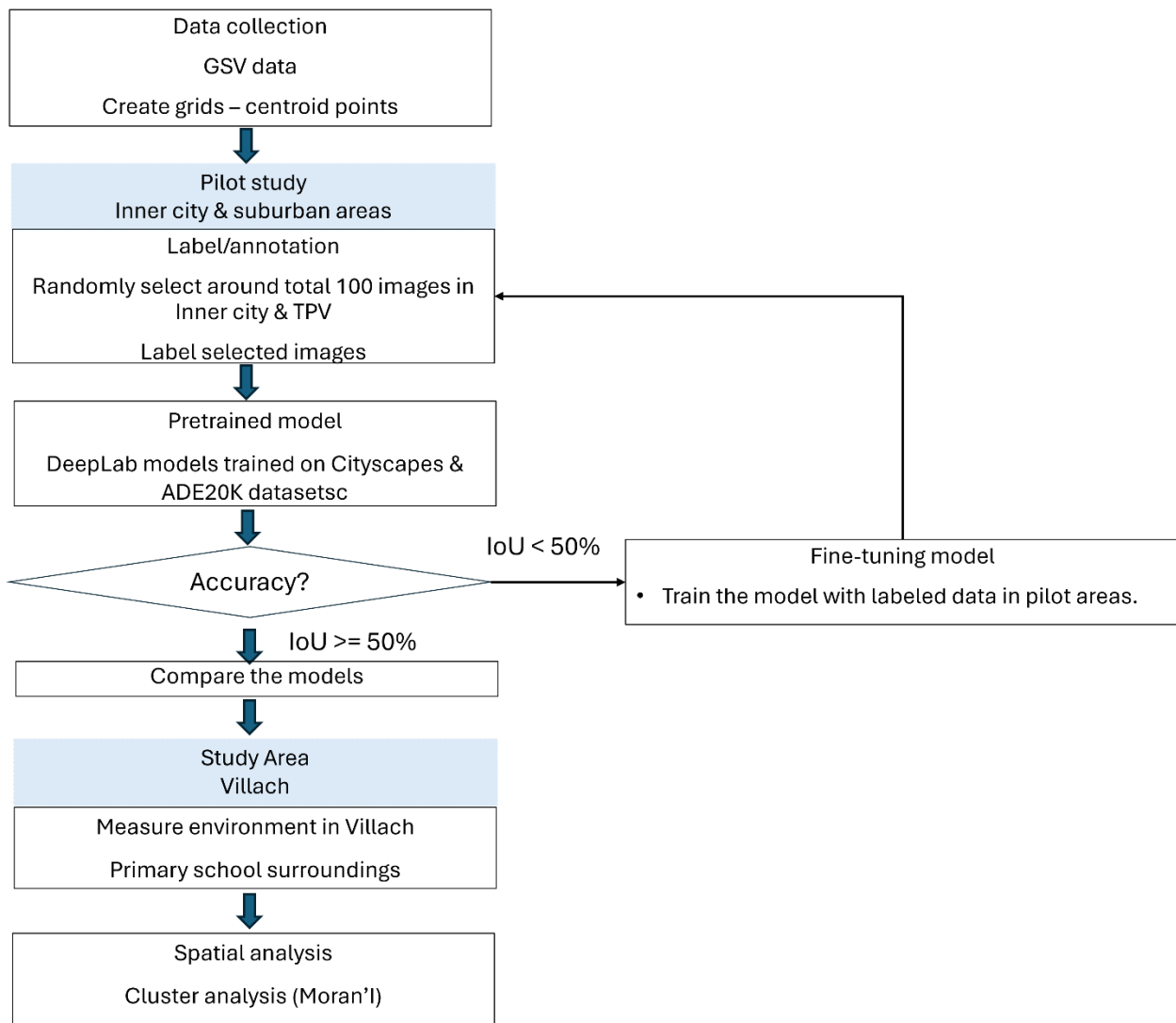
Figure 3.1 Workflow of the methodology

This workflow (Figure 3.1) highlights the critical role that pilot studies play in ensuring the accuracy and adaptability of image segmentation models before applying them to the entire study area. By selecting a small sample of images from both the city center and suburban areas, the performance of the model is tested in a local setting to account for spatial variation. Pre-trained models (e.g., DeepLabv3 model) often perform well on general datasets such as Cityscapes or ADE20K but may need to be adjusted to account for specific characteristics of the study area. Through an iterative process of random selection, labeling, accuracy calculation, and model fine-

12

tuning, the workflow ensures that the model is effectively adapted to the local environment with minimal labeled data. If the model's accuracy falls below an acceptable threshold (e.g., IoU < 50%), it is improved using additional labeled images from the pilot study. This approach reduces the labor-intensive task of large-scale labeling while ensuring that the model performs well across the entire study area. Thus, the pilot study serves as a testing ground for improved methods, balancing efficiency and accuracy before scaling up for wider application.

3.1 Data

The primary data source for this study is Google Street View (GSV) imagery, which provides comprehensive, street-level visual data for various locations worldwide. Previous studies often divided the study area into small grids, such as 50m x 50m or 100m x 100m, for downloading GSV data (Ta et al., 2021; Zhang et al., 2023). As mentioned before, GSV data offers a valuable, efficient, and widely accessible tool for objective environmental measurement. However, GSV image data also have certain limitations, such as image quality, geographic availability of imagery, and the potential for image obstructions (Rzotkiewicz et al., 2018). Image data in Google Street View (GSV) is captured using specialized cameras mounted on vehicles, which create a 360° view and are geotagged with GPS coordinates for precise location identification(Rzotkiewicz et al., 2018).

GSV has significant potential in epidemiological studies, where several issues need to be carefully addressed, including the spatial and temporal coverage of GSV and privacy concerns (Larkin & Hystad, 2019). For the spatial and temporal coverage of GSV data, not all cities have the GSV data in all streets, as urban areas are more likely to contain comprehensive GSV coverage, while rural areas or smaller streets lack GSV data (Clarke et al., 2010). In the study of 45 small- and medium-sized cities in the U.S, 44% of commute routes do not have adequate GSV image spatial coverage (Kim & Jang, 2023). Due to the characteristics of GSV data collection, GSV data

mainly cover the areas along the roads, rather than the further inner areas in neighborhood. In that case, some studies also used the areas along the roads for data collection. For instance, Li et al. (2015) randomly chose sample points along the road map. Wang et al. (2019) collected the GSV data based on the roads provided by OpenStreetMap. Meanwhile, GSV imagery data are not real time data but only show "what our cameras were able to see on the day that they passed by the location". Afterwards, it takes months to process them. This means that the content you see in GSV data could be the street view from a few months to a few years old (Google, n.d.).

3.2   Image segmentation

This study uses Deeplabv3 model, a neural network model for image segmentation to process the GSV images and classify various elements within them. Image segmentation is a technique in computer vision that divides an image into segments, each representing a specific object or background. Machine learning is a subset of artificial intelligence that focuses on developing algorithms that allow computers to learn patterns from data and make predictions or decisions without being explicitly programmed. Neural networks are a foundational technique in machine learning, inspired by the structure of the human brain, and are particularly effective for tasks like image segmentation. The DeepLabv3 model uses a spatial pyramid pooling module to emphasize contextual information at different resolutions (Chen et al., 2018). This method allows for the isolation and analysis of environmental features, including green spaces, construction, transport infrastructure, and the sky view.

Pre-trained DeepLabV3 models used in this study are available through TensorFlow Model Garden, a repository providing state-of-the-art model implementations for TensorFlow users, supporting both research and product development (Yu et al., 2020). The DeepLabV3 models in TensorFlow Model Garden have been trained on several datasets, including PASCAL VOC 2012, Cityscapes, and ADE20K datasets.

14

The PASCAL VOC 2012 dataset is derived from the large, hand-labeled ImageNet dataset, which includes 10 million labeled images across 10,000+ object categories. It categorizes images into 21 classes, covering vehicles, household items, animals, and people, with specific classes such as aeroplane, bicycle, boat, bus, car, motorbike, train, bottle, chair, dining table, potted plant, sofa, TV/monitor, bird, cat, cow, dog, horse, sheep, and person. The dataset includes images across all seasons and encompasses indoor, outdoor, and natural scenes. However, it does not specifically focus on urban environments with elements like green spaces, buildings, and roads, which limits its relevance for this study.

The Cityscapes dataset is specifically designed for urban street-view imagery, consisting of 5,000 finely annotated images and 20,000 coarsely annotated images from 50 cities across Europe, captured primarily in spring, summer, and fall. It covers 8 main groups: flat (road, sidewalk, parking, rail track), human (Person, rider), vehicle (car, truck, bus, on rails, motorcycle, bicycle, caravan, trailer), construction (building, wall, fence, guard rail, bridge, tunnel), object (pole, pole group, traffic sign, traffic light), nature (vegetation, terrain), sky (sky), and void (ground, dynamic, static), making it particularly suitable for urban analysis.

The ADE20K dataset contains over 20,000 scene-centric images with pixel-level annotations for both objects and object parts, spanning 150 semantic categories. These include background elements like sky, road, and grass, as well as individual objects such as people, cars, and furniture. Like the PASCAL VOC 2012 dataset, ADE20K offers comprehensive coverage across all seasons and includes indoor, outdoor, and natural scenes from diverse locations globally.

Given the urban focus of Google Street View (GSV) data in Villach and the study's emphasis on environmental factors such as green space, buildings, and roads, this research selects the DeepLabV3 models trained on the Cityscapes and ADE20K datasets. These models provide

greater relevance to the urban environment, allowing for accurate measurement and analysis of Villach's landscape features. By comparing the accuracy of models trained on these datasets, this study aims to identify the most suitable model for assessing the environment in Villach through the measurement of green space, constructions, transport infrastructure, and sky view.

To test the workability and accuracy of the pre-trained models, this study chooses an inner city and a suburban area (Technology Park Villach in this study) and randomly selects points in these two pilot areas. Before calculating the accuracy, it is (do not use abbreviations like this in an academic paper) necessary to label the Google Street View (GSV) images to ensure each pixel is categorized appropriately. Labeling, in this context, refers to the process of assigning specific semantic classes (such as "green space," "construction," "transport infrastructure," and "sky view") to every pixel in each image. This labeling is typically achieved through semantic segmentation using a machine learning model. Comparing the labeled images and filters predicted by models, this study uses the Intersection over Union (IoU) metric to evaluate the model's performance. IoU is a commonly used measure for segmentation accuracy, representing the overlap between the predicted segment and the actual ground truth divided by the union of both. Higher IoU values indicate better segmentation accuracy, providing confidence in the model's ability to classify environmental features accurately.

The next step is to choose the model with the highest mean IoU. Usually, models with an above 50% IoU are considered to perform well in accuracy. If the IoU is within an acceptable range, above 50%, it indicates good model performance. This model can then be used to measure environmental features across the city. If the IoU is below 50%, the labeled images will be used to fine-tune the model. This process involves adding labels and retraining the model with an additional 100 labeled images at each iteration until the model performs well within the study area.

3.3   Environment measurement

Once segmented, the GSV images are analyzed to quantify specific environmental features, focusing on four key categories: green spaces, constructions, transport infrastructure, and sky view. These features are quantified by calculating the proportion of each category in the segmented images. In this study, grids are created, and the GSV images from four cardinal directions (north, south, east, and west) are used to represent the built environment at the centroid of each grid point. Following the methodology used in GVI measurements, the average ratio of environmental elements from all four directions for each point is taken as the representative value for that point's built environment. In addition to basic proportion calculations, comparison between areas, analysis on the environment around primary schools and spatial autocorrelation analysis helps to explore the spatial pattern of the environment. This foundational analysis provides insights into how the immediate surroundings may influence children's health behaviors, and it sets the stage for future research on environmental disparities and the relationship between children's health and their environment.

4   A case study in Villach, Austria

This chapter will apply the methods described in the previous section, utilizing green space, construction, transport infrastructure, and sky view to represent the environmental characteristics of Villach. The objective of this case study is to evaluate the environment in Villach through a grid system of 100m x 100m cells, resulting in a comprehensive dataset of 13,502 sampling points. Two representative pilot areas are selected for analysis: the inner city (Innere Stadt), which is characterized by higher population density and vibrant commercial activity, and the Technology Park Villach (TPV), an area with lower population density that contains Carinthia University of Applied Sciences and other small private companies.

Section 4.1 briefly introduces the study area Villach and data collection. Section 4.2 focuses on the selection of pre-trained models, specifically the ability and accuracy applying DeepLabv3 model in pilot areas. Section 4.3 compares the environment in two distinct pilot areas. Following this, Section 4.4 delves into the citywide environment in Villach. Finally, Section 4.5 discusses spatial analysis to deeply understand the spatial distribution of the environment.

4.1   Study area and data

Villach is a city in southern Austria, located in the state of Carinthia, near the borders with Italy and Slovenia. It is the second-largest city in Carinthia, with a population of around 65,000. Positioned along the Drava River, Villach is framed by mountain ranges, with the Karawanks to the south and the Villach Alps to the west.

To systematically assess GSV data in Villach, a grid system with 100m x 100m cells is created using ArcGIS Pro, resulting in a total of 13,502 cells. Each cell's centroid serves as a sample point for capturing the surrounding environment. GSV images are downloaded from Google Maps API at each centroid location in four cardinal directions - north (0°), east (90°), south (180°), and west (270°) - to provide a comprehensive 360-degree view (Figure 4.1). GSV's camera field of view is approximately 90 degrees, ensuring that the four directional images collectively cover the entire panoramic perspective.

north (0°)   east (90°)   south (180°)   west (270°)
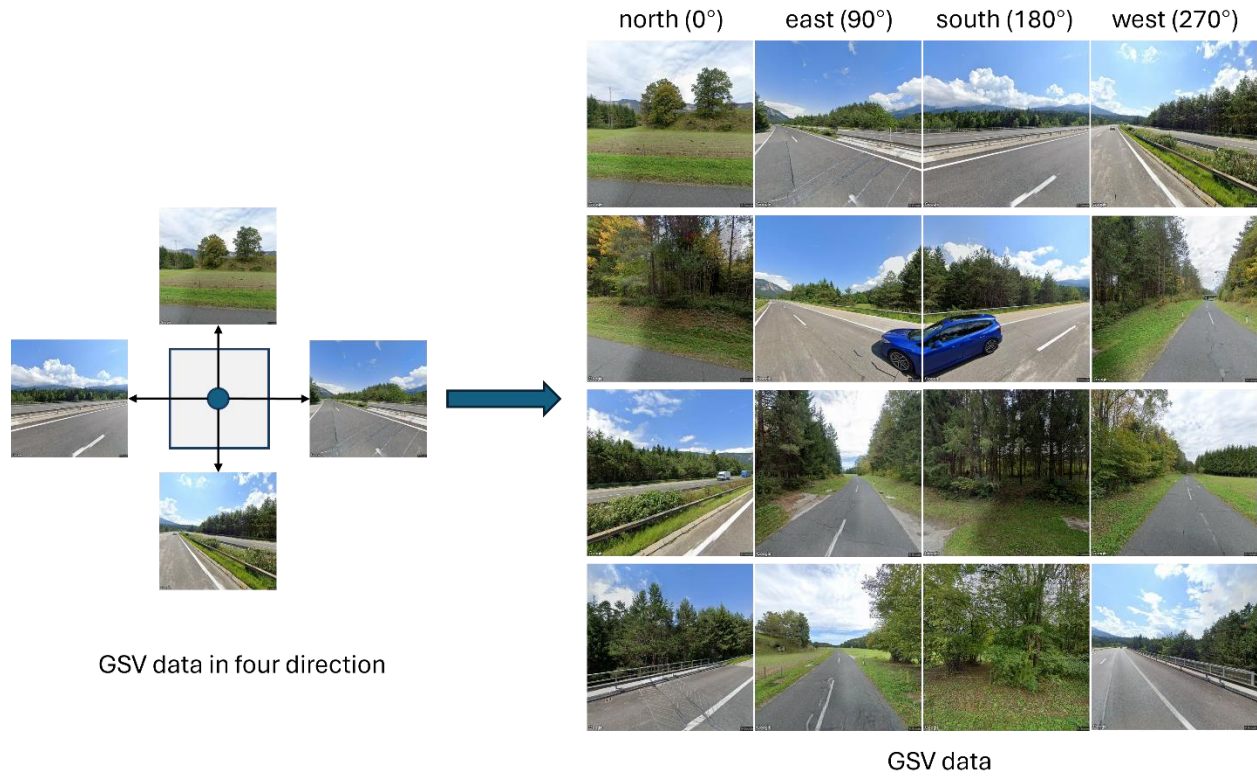
GSV data in four direction

GSV data

Figure 4.1 GSV data collection in four directions and samples of GSV data in Villach

Among the 13,502 points, 10,080 points lack GSV data, and 1 point has GSV data available in only two directions. Of the initial points, 3,421 points that are primarily located in urban areas and near roadways have complete GSV coverage in all four directions, resulting in a total of 13,684 images. As shown in Figure 4.2, GSV data is concentrated in the central areas, while there is a lack of GSV data for the mountainous areas, as well as the internal neighborhoods beyond the major roads, where Google Street View vehicles may not be able to access or may not have recorded data.
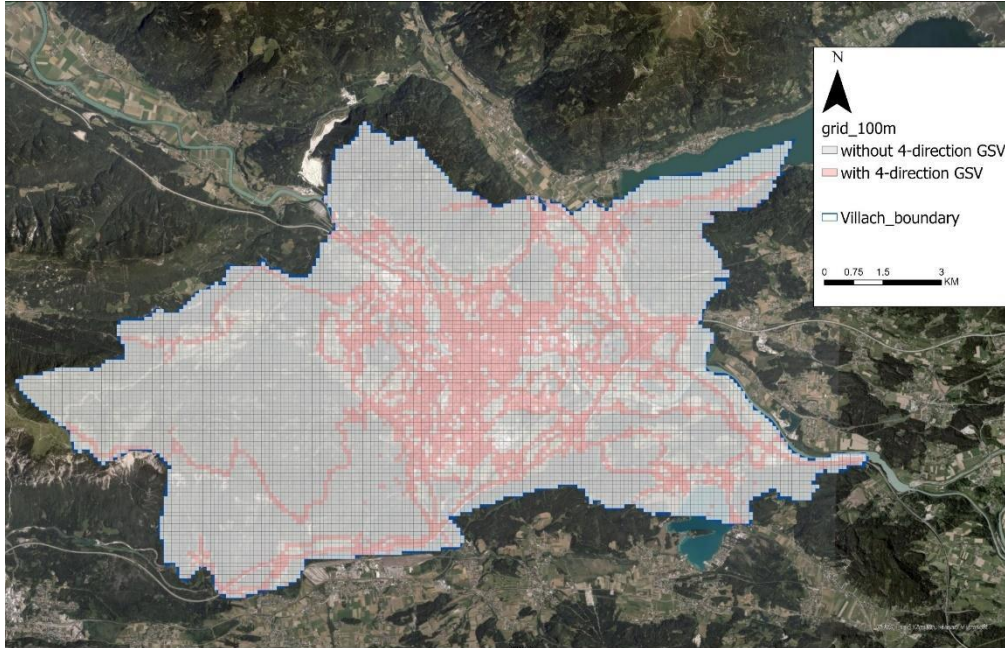
Figure 4.2 The coverage of GSV data in Villach, Austria

Among the 3,421 points, 3 points have no available GSV images, and 5 points produce low-quality images, which were likely caused by locations in tunnels, underground parking areas, or other obstructed environments where the view does not accurately represent the outdoor environment. To address these issues, the study selects high-quality street view images to assess the environment in Villach. Ultimately, 3,413 points, comprising a total of 13,652 GSV images, are included as data for this study (Figure 4.3). The collected GSV data for Villach span from January 2014 to July 2024, with a significant portion (2,041 points, or 59.8%) gathered in 2023 (Table 4.1).
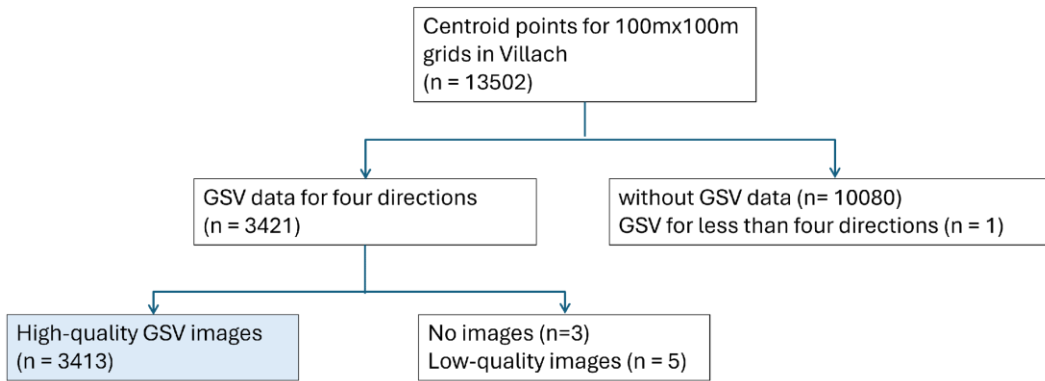
Figure 4.3 Workflow of GSV Data Preprocessing and Selection

Table 4.1 Temporal coverage of GSV data in Villach

Year	Frequency
2014	2
2015	12
2016	11
2017	27
2018	214
2019	413
2020	145
2021	244
2022	298
2023	2041
2024	6
Total	3413

To examine the locations of primary schools in Villach and measure the surrounding environment, primary school data is downloaded from OpenStreetMap using the Python OSMnx package (Boeing, 2017). After data cleaning, a total of 31 records are retained. Most of the primary schools are concentrated in central areas and the southern regions of Villach (Figure 4.4).
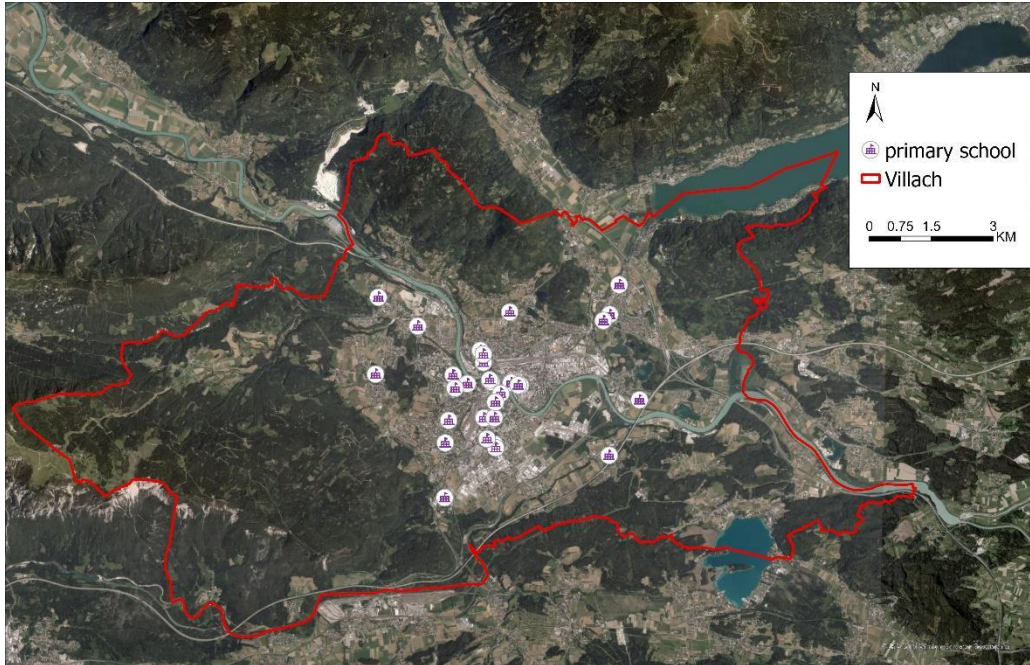
Figure 4.4 Primary schools in Villach, Austria (Data from OpenStreetMap, downloaded Aug.2024)

4.2   Selection of pre-trained models

In this study, pre-trained DeepLabv3 models are employed to classify various aspects of the environment in Villach using GSV data. The DeepLabv3 model is a neural network architecture specifically designed for semantic image segmentation, enabling it to accurately identify and classify different elements within images.

To assess the accuracy of the pre-trained DeepLabv3 models in the context of Villach and to select the most appropriate model, two pilot areas were chosen: the inner city (Innere Stadt) around the Villach central station (Villach Hbf) and areas around the Technology Park Villach (TPV). The inner city is the central area of Villach, characterized by a higher population density, numerous stores, and various facilities. In contrast, TPV is located approximately 3km from the city center and exhibits a lower population density, containing Carinthia University of Applied Sciences (FH Kärnten) and several technology companies. The inner city pilot area contains 133

points, of which 126 have complete image data in all four directions. The Technology Park Villach (TPV) pilot area consists of 136 points, with 75 points providing complete four-directional image data. Therefore, in the inner city, 126 points contribute a total of 504 images (126 x 4), while in TPV, 75 points contribute 300 images (75 x 4), resulting in a total of 804 images across both pilot areas. These images (rather than centroid points) are used in the analysis.

These areas are selected based on the assumption that they present distinct environmental characteristics due to their differing land uses (Figure 4.5). The inner city, with its dense urban fabric, is expected to showcase more construction and transport infrastructure, while the less urbanized surroundings of TPV may reveal a higher proportion of green spaces. Furthermore, these pilot areas allow for the evaluation of the robustness and performance of different pre-trained models, including variations of the DeepLabv3 model trained on diverse datasets. The contrasting environments of the inner city and TPV pose a challenge for the model, as it must accurately classify and segment different elements within the images. This approach provides a comprehensive evaluation of the model's capabilities.
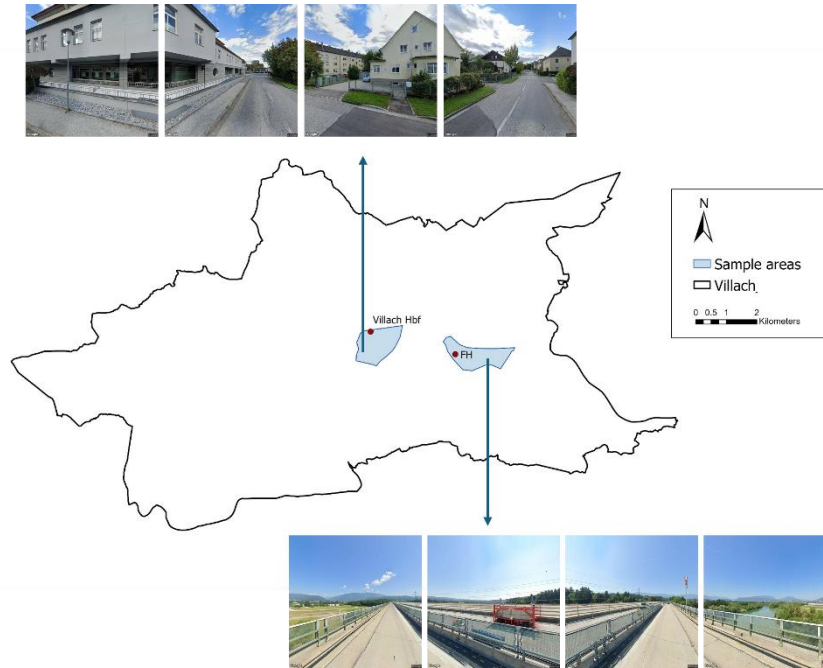
Figure 4.5 Pilot areas for testing the pre-trained models: the inner city and the TPV

First step is to test the workability of the two pre-trained models in the pilot areas and compare the differences between these two pre-trained models. After the image segmentation and calculating the environmental factor ratios for each of the four directions at each centroid point, table 4.2 represents the average ratios (%) for green space, construction, transport infrastructure, and sky for both models (ADE20K and Cityscapes) in pilot areas. ADE20K and Cityscapes, exhibit comparable values across the four categories within the context of Villach. Specifically, the model trained on Cityscapes demonstrates a higher average green space ratio (23.09%) compared to the model trained on ADE20K (18.68%), while also displaying elevated construction (30.55%) and transport infrastructure (26.77%) ratios. However, Cityscapes model shows a lower sky ratio (16.13%) compared to ADE20K model (23.88%).

When examining the pilot areas, ADE20K model has a lower average construction ratio (28.93%) than Cityscapes model (34.17%) in inner city, whereas in the TPV area, Cityscapes

model shows a more substantial green space ratio (31.20%) compared to ADE20K model (27.82%). This comparison suggests that while both models can be applied to Villach, their performance varies by area and category, indicating potential strengths and weaknesses in environmental segmentation tasks.

Table 4.2 Output of different environmental features by pre-trained models in Villach's inner city and the TPV (%)

	Overall (n=201)		Inner city (n = 126)		TPV (n = 75)	
	Cityscapes	ADE20K	Cityscapes	ADE20K	Cityscapes	ADE20K
Green space	23.09	18.67	18.27	13.24	31.20	27.82
construction	30.55	22.41	34.17	28.93	24.46	11.45
Transport Infrastructure	26.77	24.39	27.77	25.57	25.10	22.41
sky	16.13	23.88	15.11	19.61	17.85	31.06

To further investigate the applicability of these models and ascertain whether the observed differences in ratios are statistically significant, t-tests are employed to compare the means across models and the built environments categories.

As shown in Table 4.3, almost all the built environment factors in pilot areas indicate the statistically significant differences between the ADE20K and Cityscapes models, except for green space in the TPV area and transport infrastructure in the inner city. Specifically, the ADE20K model serves as the reference, the Cityscapes model yields lower mean values for green space, construction, and transport infrastructure ratios while producing a higher mean sky ratio than the ADE20K model across the combined dataset and within each pilot area. Given the large sample sizes (n = 201, 136, and 75), the t-test's robustness is justified by the central limit theorem even when the population distributions, from which the three samples are drawn, would not show a

normal distribution. The results of the t-tests have indicated that there are significant differences between the two models in certain areas, particularly in construction and transport infrastructure ratios and sky ratios.

These significant differences suggest that the underlying training dataset has a substantial impact on each model's segmentation, particularly in categories like green space and sky where environmental factors exhibit high variability. This underscores that model choice, influenced by the training data, may introduce a bias or uncertainty in environmental segmentation applications, highlighting the importance of selecting datasets that align closely with the intended analysis environment to achieve consistent and reliable segmentation interpretations.

Table 4.3 T-Test results comparing ADE20K and Cityscapes models

	Overall (n=201)		Inner city (n=136)		TPV (n=75)	
	t-statistic	p-value	t-statistic	p-value	t-statistic	p-value
Green space	-2.771	0.006**	-2.954	0.003**	-1.277	0.203
construction	-4.353	0.000***	-2.111	0.036*	-5.945	0.000***
Transport Infrastructure	-2.437	0.015*	1.628	0.105	-2.126	0.035*
sky	7.401	0.000***	3.557	0.000***	8.858	0.000***

Significant: *: p<0.05; **: p<0.01; ***: p<0.001.

Secondly, to evaluate the accuracy of the models applied in these two pilot areas and facilitate potential fine-tuning, this study randomly selected approximately 100 images, annotating 52 street view images from 13 points in each pilot area. In total, 104 street view images were annotated using LabelMe, a graphical image annotation tool developed in Python with a Qt-based interface (Wada, n.d.). This annotation step is crucial for testing, training, and refining the pre-trained DeepLabv3 models.

Referring to the classifications of both the Cityscapes and ADE20K datasets, the elements in these images have been categorized as follows: green spaces (vegetation and grass), constructions (buildings, fences, and walls), transportation infrastructure (roads, sidewalks, and parking areas), and sky.

While both datasets (Cityscapes and ADE20K) feature street view images with similar classifications, they differ in their specific class definitions. For instance, the Cityscapes dataset categorizes all plants as vegetation, whereas ADE20K distinguishes between trees, flowers, and other types of flora. Additionally, Cityscapes combines grass and fields under a single class called "terrain," while ADE20K treats them separately. This lack of precise alignment complicates matching classifications in detail. However, this study focuses on broader environmental categories—such as the green space index—rather than the specific subclasses under green space, as these detailed distinctions do not significantly affect the overall environmental measurements. Consequently, when calculating accuracy, this study computes the Intersection over Union (IoU) for these broader groups instead of individual classes.
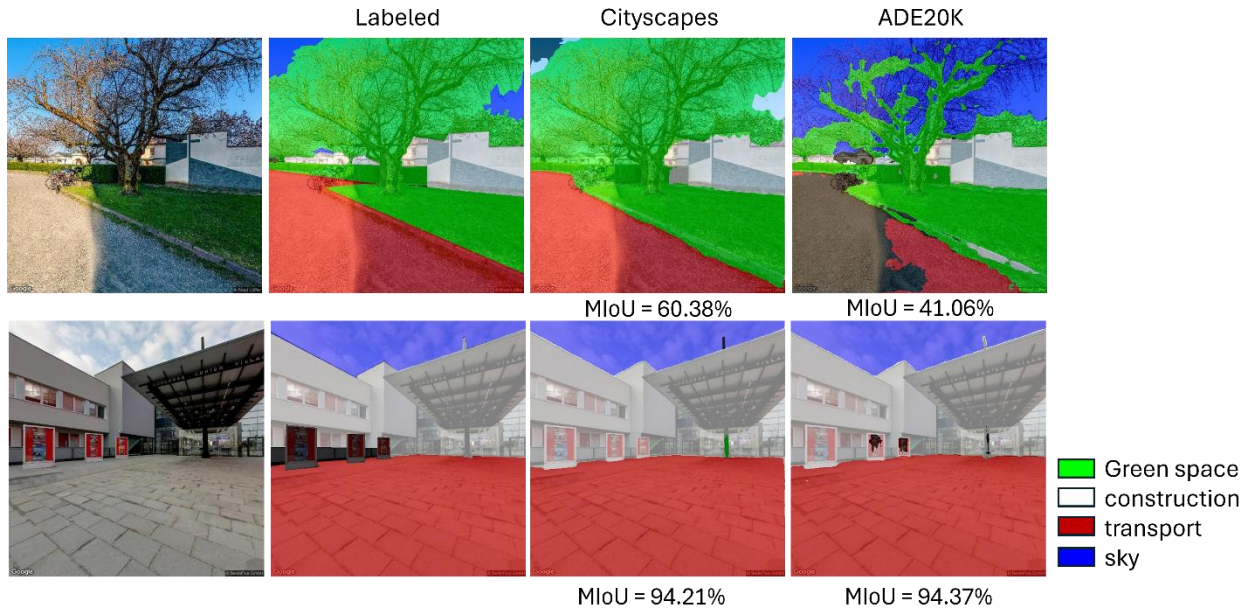
Table 4.4 displays the Intersection over Union (IoU) accuracy scores for two semantic segmentation models, Cityscapes and Ade20k, across green space, construction, transport infrastructure, and sky categories in two pilot areas. Both models demonstrate better performance in the inner city compared to Technology Park Villach (TPV). The Cityscapes model demonstrates high segmentation accuracy within the inner city, culminating in an overall mean IoU (MIoU) of 78.75%. TPV also yields robust results with Cityscapes model, particularly in transport infrastructure (88.15%) and green space (83.98%), although construction and sky classes show comparatively lower accuracy at 34.24% and 61.23%, resulting in an MIoU of 66.90%. The ADE20k model delivers generally high segmentation accuracy in the inner city as well, yielding

an MIoU of 82.62%. TPV performance with ADE20k also shows strong green space accuracy, contributing to an MIoU of 78.57%. Overall, both models exhibit satisfactory accuracy(>50%) across classes in both urban and suburban environments, indicating that these models can be confidently deployed in these settings without further fine-tuning.
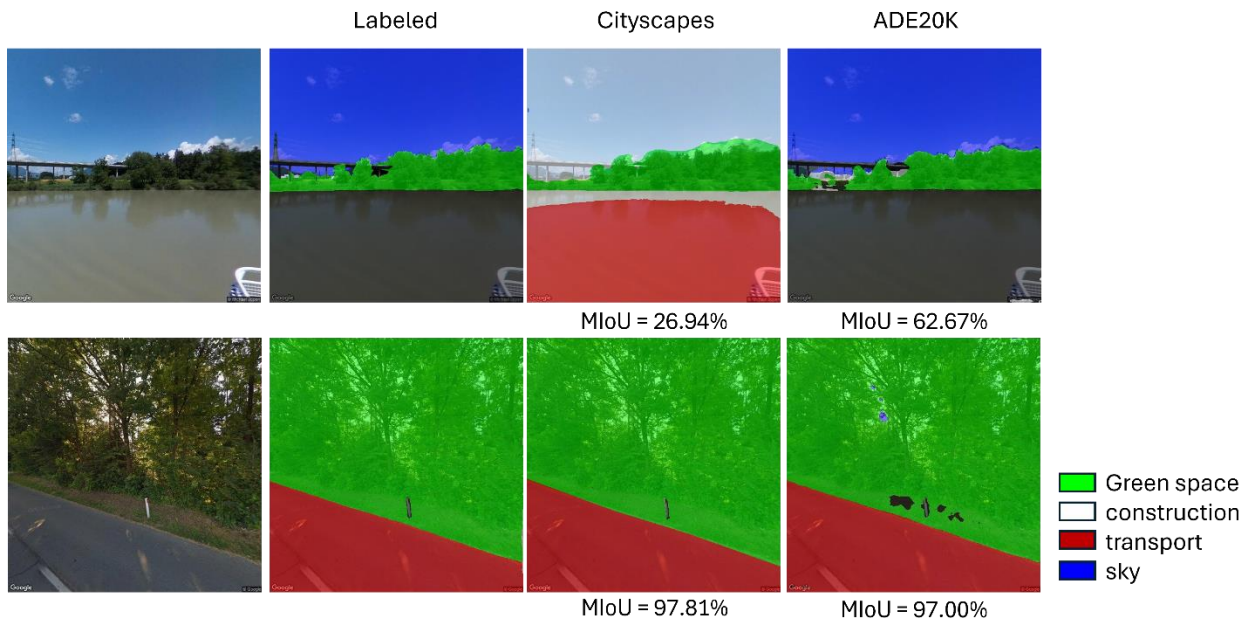
Table 4.4 The Intersection over Union (IoU) accuracy scores(%) for two models in pilot areas

models	Pilot areas	green space	construction	Transport Infrastructure	sky	MIoU
Cityscapes	Inner city	74.88	78.12	87.46	74.51	78.75
	TPV	83.98	34.24	88.15	61.23	66.90
Ade20k	Inner city	72.97	83.76	82.36	91.39	82.62
	TPV	88.23	55.67	79.08	91.28	78.57

Figure 4.6 displays the results of image segmentation applied to both the inner city and TPV pilot areas, showcasing classification outputs with the highest and lowest mean Intersection over Union (MIoU) scores. After calculating the mean value from the MIoU two models (Cityscapes and ADE20K), these images represent the highest and lowest average MIoU values in each pilot area, showing the classification outputs with the best and worst overall segmentation performance. It is also indicated that both models, trained on the Cityscapes and ADE20K datasets, perform better in the inner city compared to the TPV area. Additionally, images with fewer classes and less overlap tend to exhibit higher segmentation accuracy.

Labeled	Cityscapes	ADE20K
	MIoU = 60.38%	MIoU = 41.06%
	MIoU = 94.21%	MIoU = 94.37%

Green space
construction
transport
sky

a) Inner City with Low and High MIoU

Labeled	Cityscapes	ADE20K
	MIoU = 26.94%	MIoU = 62.67%
	MIoU = 97.81%	MIoU = 97.00%

Green space
construction
transport
sky

b) TPV with Low and High MIoU

Figure 4.6 Sample classification outputs from Cityscapes and ADE20K models in pilot Areas

The street view images in TPV are often obscured by vegetation, distant mountains, and sky. Furthermore, since the Cityscapes dataset predominantly features urban street view imagery, this focus may contribute to lower accuracy in areas with relatively low urbanization. Figure 4.7

demonstrates examples from TPV with low and high IoU scores for construction detection, comparing both models' outputs. The accuracy results from the left image (low IoU) are shown in the first IoU column, while the results from the right image (high IoU) are shown in the second IoU column. These differences highlight the challenges in detecting construction areas, which occupy a smaller visual space than other environmental features, suggesting a need for model fine-tuning with locally relevant data for improved performance in suburban or rural landscapes like TPV. The images indicate that construction areas in TPV occupy a smaller visual space than green spaces and other environmental elements, which may lead to these areas being overlooked or misclassified by the models. This suggests a potential need for model adaptation or fine-tuning using locally relevant data to improve performance in suburban or rural landscapes like TPV.

TPV	IoU	IoU
Cityspaces	0	94.23%
Ade20K	17.31%	84.56%

Figure 4.7 Example from TPV showing low (left) and high (right) IoU scores for construction

4.3   Comparison between inner city and TPV

In the previous session, two pilot areas have been labeled to evaluate the accuracy of the pre-trained models. Both models, trained on the Cityscapes and ADE20K datasets, performed well in the context of Villach; however, the model trained on the ADE20K dataset exhibits higher

accuracy. Therefore, this study utilizes the ADE20K-trained model to classify street view images for environmental measurements.

As previously mentioned, the inner city and TPV exhibit differences due to their distinct locations and land uses. This study further investigates the statistical differences between these two areas. As shown in Table 4.5, while the mean of transport infrastructure ratios is similar between the inner city and TPV, differences exist in green space, construction, and sky view. The inner city has a slightly higher average transport infrastructure ratio (0.254) compared to TPV (0.220), likely due to the nature of the GSV data, which are primarily collected along roadways.

TPV boasts a significantly higher mean green space ratio (0.277) than the inner city (0.133), with a comparable median, indicating more consistent green space coverage in TPV. However, the variability in green space is slightly greater in TPV, suggesting a diversity in green space availability. In terms of construction, the inner city exhibits a higher mean construction ratio (0.290) compared to TPV (0.116), with a broader range in the inner city reaching up to 0.860, whereas TPV peaks at 0.510. Furthermore, TPV has a higher mean sky ratio (0.310) compared to the inner city (0.196), implying a more open environment with fewer tall buildings. The inner city's lower sky ratio aligns with an environment surrounded by more vertical structures.

These findings support the assumption that TPV retains characteristics of suburban spaces: more green coverage, lower building density, and higher sky visibility. In contrast, the inner city has denser construction and road infrastructure, which limit both green space and sky visibility. This comparison highlights that TPV's landscape is more open and potentially more conducive to outdoor activities, in contrast to the more enclosed and built-up environment of the inner city.

Table 4.5 Comparison of the environment between inner city and TPV using ADE20K-trained model

		Mean	SD	Median	Min.	Max.
Inner city	Green space	0.133	0.12	0.1	0	0.63

	Construction	0.29	0.167	0.245	0.019	0.86
	Transport Infrastructure	0.254	0.118	0.28	0	0.46
	Sky View	0.196	0.107	0.21	0	0.435
TPV	Green space	0.277	0.152	0.28	0.008	0.6
	Construction	0.116	0.112	0.084	0.0001	0.51
	Transport Infrastructure	0.22	0.084	0.227	0	0.41
	sky	0.31	0.097	0.32	0	0.45

Figure 4.8 displays the results of four categories of built environment in both inner city and TPV. Compared with the previous descriptive analysis, the maps display a more direct visual of the differences between inner city and TPV. To have a clear visualization, all legends use the same range of the value taking the range of TPV as reference. It is obvious that the inner city has more construction and transport infrastructure, while TPV contains more green space and sky that indicates a more beneficial environment to children's health behavior.

In the Inner city (left-side maps), the maps show a relatively dense distribution of construction coverage, with notable amounts of transport infrastructure. This reflects the typical urban landscape, where construction and roads are more dominant features. Green space is less prominent in this area. Sky visibility also appears restricted, with mid-range values that suggest a moderate density of open views.

On the other hand, the TPV area (right-side maps) exhibits a contrasting spatial pattern. Green space occupies a more significant portion, with many darker symbols spread across the region, indicating higher proportions of vegetation or open, undeveloped land. Construction density is visibly lower in TPV compared to the Inner city, with fewer dark symbols in this category, reflecting the suburban character of the technology park. Transport infrastructure is present but generally lighter than in the Inner city, suggesting a less complex road network in TPV,
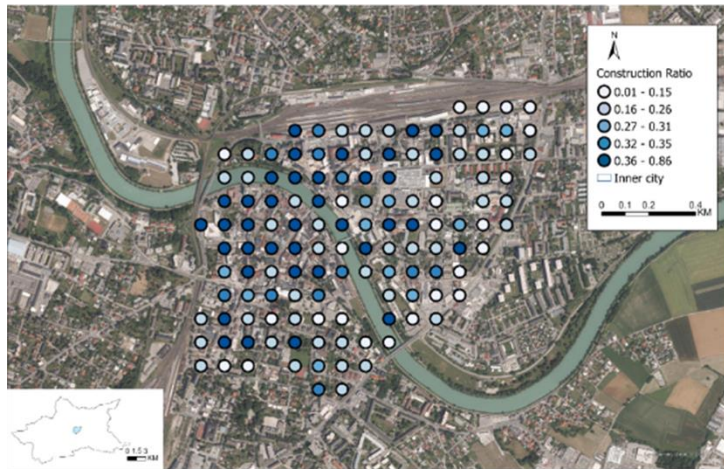
which aligns with its suburban function where high-density road networks are less necessary. Sky visibility in TPV is higher than in the Inner city, likely due to the lower density of tall structures.
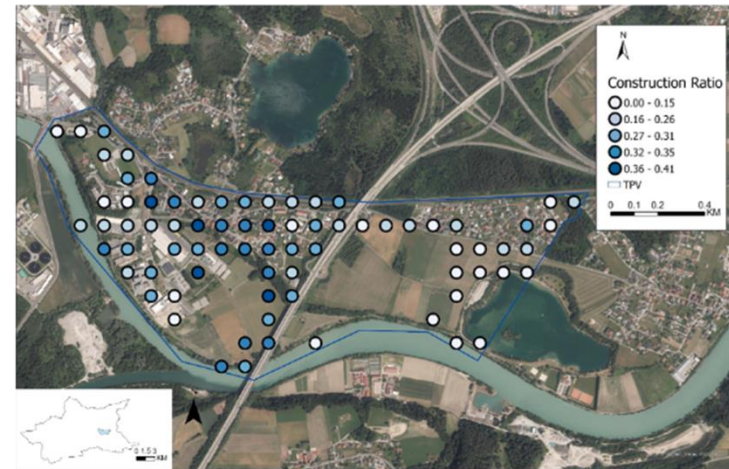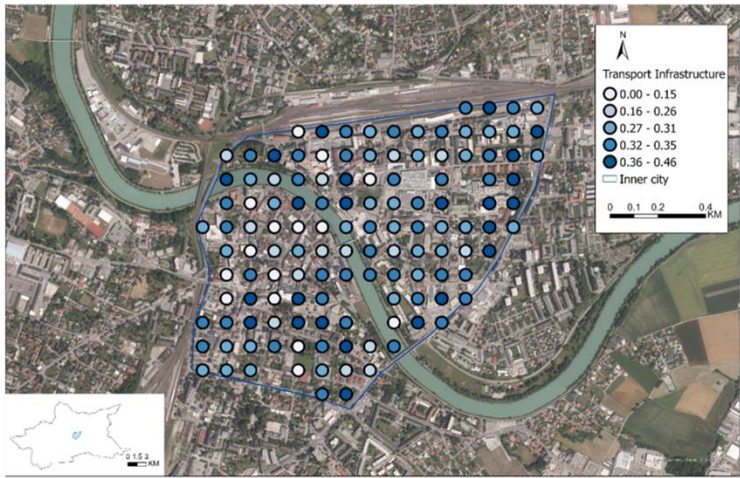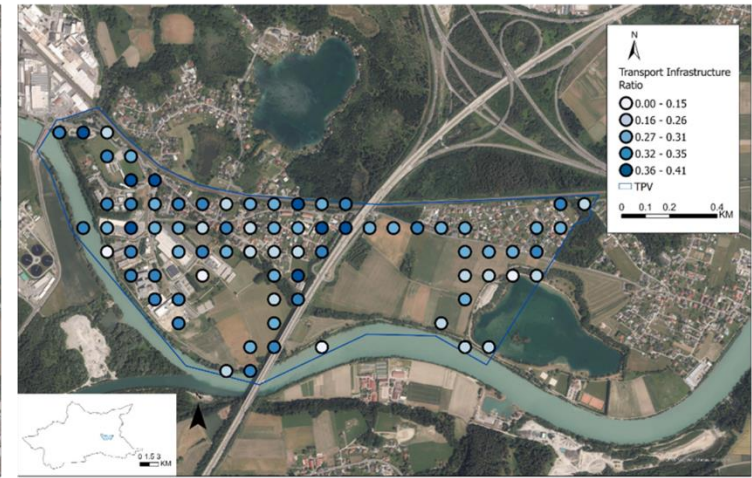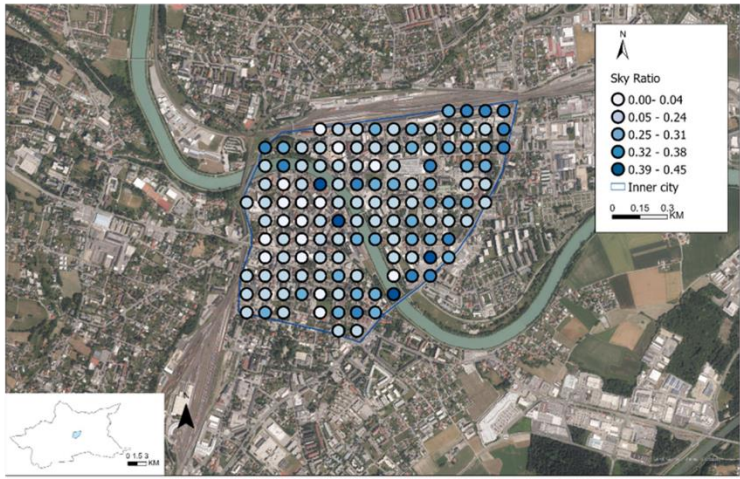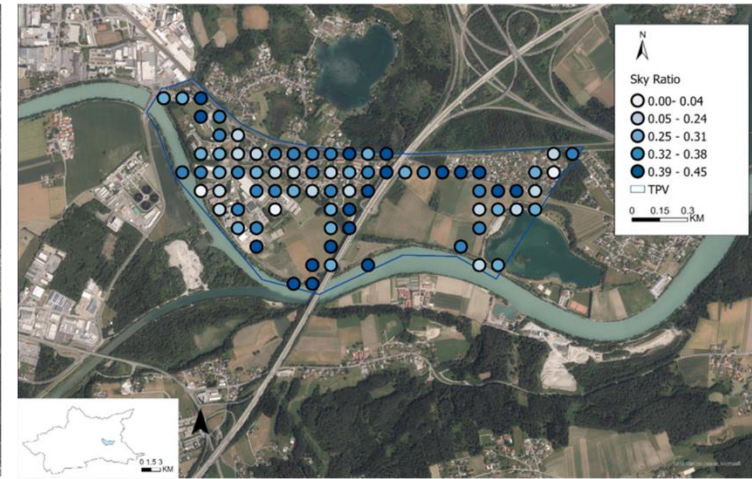
a

e

b

f

34
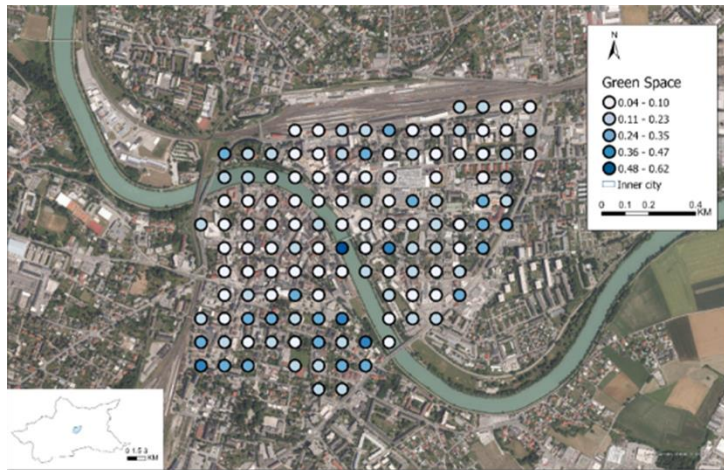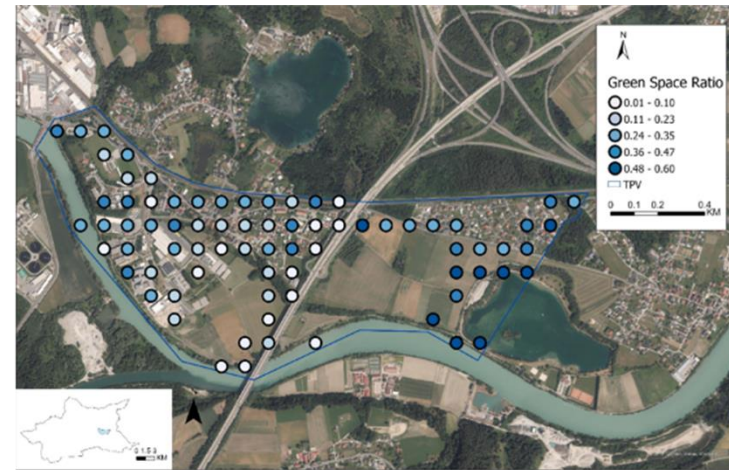
Figure 4.8 Environmental indicators in two pilot areas: a-d depict green space, construction, transport infrastructure, and sky view in the inner city, while panels e-h illustrate the same indicators for TPV.

This comparative mapping highlights the environmental and structural differences between urban and suburban settings. The Inner city's higher construction and transport ratios and lower green space and sky visibility reflect a typical urban core's compact and developed environment. In contrast, TPV's higher green space and sky visibility and lower construction density embody the open, less congested landscape of suburban areas. This contrast in environmental makeup between the two areas provides insights into the implications of urban form and function on street-view perceptions.

The independent t-test analysis reveals significant differences in the mean ratios of green space, construction, transport infrastructure, and sky view between the two pilot areas, Inner city and TPV (Table 4.6). The mean green space ratio in TPV is significantly higher than that in the Inner city. This may be attributable to TPV's suburban landscape, which likely includes more open areas than the urbanized Inner city. In terms of construction ratio, it suggests that the Inner city has a substantially higher average construction ratio than TPV. This finding aligns with the dense urban fabric typically observed in city centers, where built environments are more concentrated, contrasting with TPV's lower-density, mixed-use suburban setting, where construction spaces are less dominant relative to green space and open areas. For transport infrastructure, it points to a statistically significant difference between Inner city and TPV with a less pronounced effect size than the other variables. The Inner city's slightly higher transport infrastructure reflects a higher density of roads and sidewalks in urban centers. This relatively smaller difference in transport infrastructure ratios between the two areas may be caused by the characteristics of GSV data that are collected along the street. It could also suggest that TPV has adequate transport provisions, given its suburban function as a technology park that may require substantial infrastructure. Lastly, the sky view shows a strong and statistically significant difference, with TPV displaying a much

higher sky view than the Inner city. This finding suggests that TPV, as a less densely constructed

suburban area, allows for more open views of the sky, whereas the Inner city's higher construction

ratios limit sky visibility.

Overall, these findings indicate the spatial disparities of the environment in Villach.

Meanwhile, as the output of deeplabv3 model trained on ADE20K datasets, it also highlights the

model's sensitivity to environmental features in each area. It implies how geographic and

functional characteristics of urban versus suburban environments are reflected in the segmentation

outputs of deeplabv3 model trained on ADE20K datasets. The statistically significant differences

in all ratios highlight the model's sensitivity to environmental features in each area, suggesting the

importance of context in model application and the influence of local environmental characteristics

on segmentation results.

Table 4.6 T-test results in two pilot areas

	t-statistic	p-value
Green space	-6.925	0.000***
construction	8.793	0.000***
Transport Infrastructure	2.156	0.032*
Sky view	-7.781	0.000***
Significant: *: $p<0.05$; **: $p<0.01$; ***: $p<0.001$.		

4.4   Spatial Distribution of Environmental Features in Villach

Using the DeepLabv3 model trained on the ADE20K dataset, this study analyzes the

environment in whole Villach using Google Street View (GSV) image data. Table 4.7 presents the

calculated proportions of four environmental indicators—green space, construction, transport

infrastructure, and sky view—expressed as percentages (%) in relation to the total area analyzed

through GSV images in Villach. There is a relatively positive presence of greenery in Villach.

Construction, with a mean of 9.6%, shows a wide range (0 to 92.0%), reflecting diverse building

densities in various parts of the city. Transport infrastructure indicates a well-developed road

network, which may facilitate mobility for children but could also expose them to traffic. The sky view ratio suggests a fair amount of open space above the urban structures. Overall, Villach's environment appears moderately conducive to children's health, given the substantial green space and open sky view. These features can support physical activity, exposure to natural elements, and overall well-being, while the balanced transport infrastructure offers accessible mobility.

Table 4.7 Environmental factor percentages (%) based on GSV images for the entire city of Villach (n = 3413)

	Mean	SD	Median	Min.	Max.
Green space	32.1	17.9	30.5	0	86.6
Construction	9.6	11.8	5.6	0	92.0
Transport Infrastructure	23.2	9.8	23.7	0	47.6
Sky View	27.2	10.9	28.8	0	49.0

Figure 4.9 displays the environment in Villach, and primary school locations are marked on each map to provide context on areas potentially frequented by children. Generally, green space tends to increase from the city center toward the boundary, while construction is more concentrated in the urban core and gradually decreases toward the outskirts. Transport infrastructure and sky visibility do not exhibit a clear spatial trend across the map.

Green space, with higher percentages clustered around the outskirts of Villach, aligns with the satellite base map. This shows that natural or vegetated areas are more common in the periphery, while the green areas are the least in the central urban area. In contrast, construction is concentrated in the urban core, indicative of denser building presence and infrastructure. The sky view is higher in areas with less built density—mainly in the outskirts and open spaces—and is lower in central areas, where tall buildings likely obstruct the sky. Transport infrastructure density shows higher values along major roads and transportation routes, reflecting areas with more extensive street networks.

Collectively, these maps reveal Villach's spatial composition, with denser urban development and infrastructure in the core and greener, more open areas in suburban and rural regions. The presence of primary schools across different environments highlights the variation in children's surroundings, which may have implications for accessibility to green spaces and exposure to urban infrastructure. Villach's primary school locations, marked on each map, reveal insights into the distribution of educational facilities relative to environmental characteristics. Many schools are located near or within urban areas, where construction density is higher and green space is relatively limited. This positioning may indicate that children in the city center have limited direct access to natural areas, potentially affecting opportunities for outdoor play and interaction with green spaces.
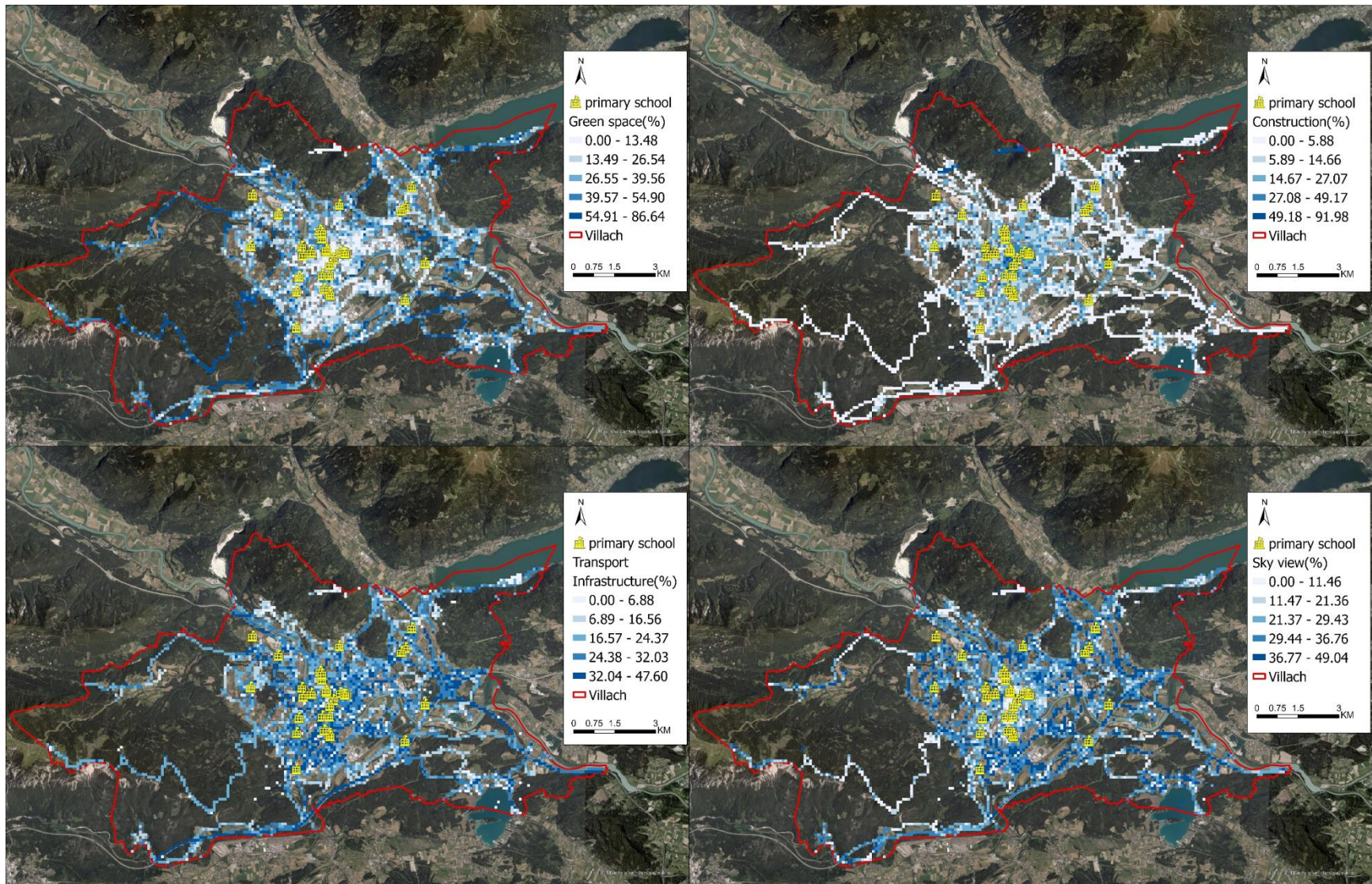
Figure 4.9 Spatial distribution of green space, construction, transport infrastructure, and sky view in Villach with primary school

This study examines the environment around 31 primary schools in Villach within five buffer zones: 100m, 200m, 500m, 1000m, and 1500m. Figure 4.10(a) illustrates these buffer ranges. Based on previous studies, a case study in London, Bosch et al. (2020) classified the walking distance as 0-500m, 500-1000m, 1000m-1500m and above 1500m, and found that different walking distances can influence children's active commuting behaviors. Missbach et al. (2017) defined the walking distance as 950m for children in a case study in Vienna. In this study in Villach, the 100m and 200m buffers are considered the closest environments around schools, due to the lack of Google Street View (GSV) data within the 100m radius for one school. The 1500m buffer represents a broader area for active commuting, such as walking and cycling, and covers a larger scope of the surrounding environment. Figure 4.10(b) shows how environmental features change with increasing distance, with construction ratios decreasing and sky view ratios increasing, reflecting the more urbanized nature of areas closer to schools.

It is important to note that the 1500m buffer in Villach includes areas such as remote mountainous and forested zones, which may not be typical walking distances for children. Therefore, the feasible walking distance for children in Villach might be shorter than in other cities, where more urbanized settings are common. This buffer analysis provides a foundation for future studies exploring how the surrounding environment at varying distances affects children's health behaviors and outcomes.
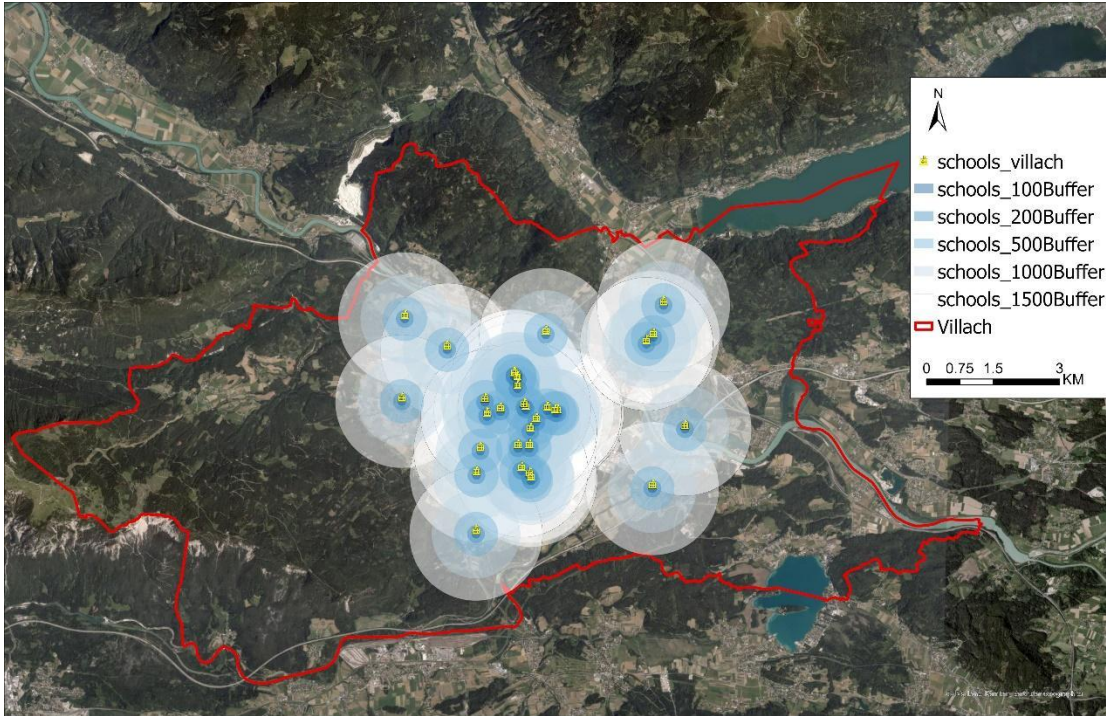
a)100m, 200m, 500m, 1000m and 1500m radius range around schools in Villach
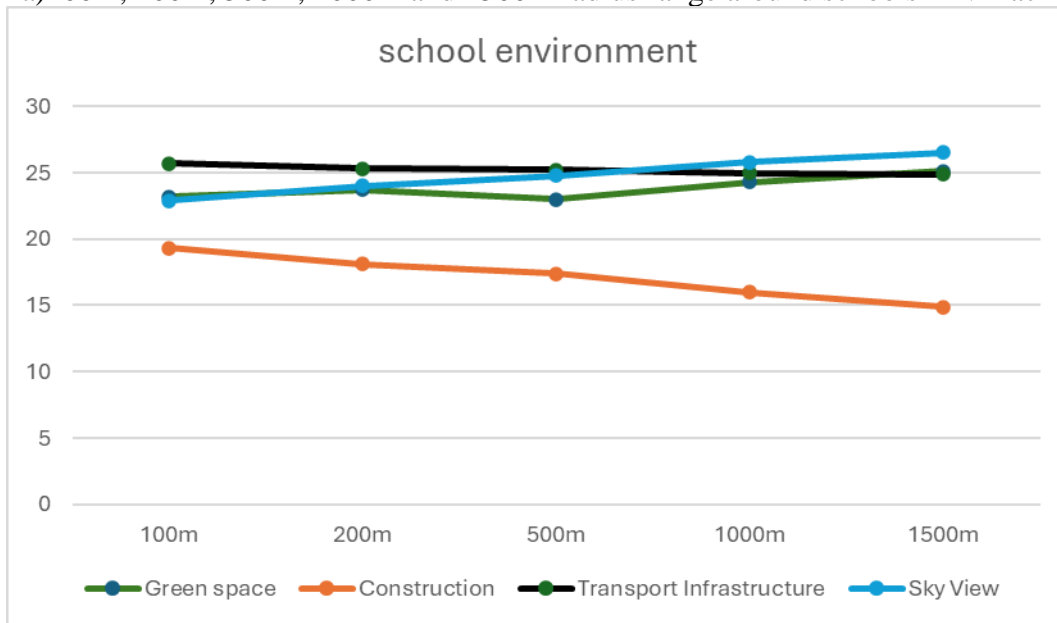
b) school environment within different range

Figure 4.10 School environment within 100m-1500m distance

Table 4.8 presents the environmental feature ratios surrounding 31 primary schools in Villach. A comparison with Table 4.7 shows that the environments around primary schools

generally reflect the citywide averages, with some notable differences. Green space around schools ranges from 23.7% to 25.1%, which is slightly lower than the citywide average of 32.1%, indicating fewer green areas near school zones. Construction coverage around schools is relatively higher, consistent with the fact that most primary schools are situated in more urbanized, central areas, leading to higher building density. Ratios for transport infrastructure and sky view are similar in both the primary school areas and the citywide averages. These findings suggest that, while the environments around primary schools share general characteristics with the broader city, they are characterized by denser construction and somewhat reduced green space, likely due to their central locations. This could limit children's access to natural spaces and emphasizes the need for targeted green infrastructure in urban school zones to support outdoor play and physical activity.

Table 4.8 Built environment around primary schools in Villach

	Green space		Construction		Transport Infrastructure		Sky View	
	Mean	SD	Mean	SD	Mean	SD	Mean	SD
100m(n=30)	23.2	8.6	19.3	11.1	25.7	4.9	22.9	6.7
200m(n=31)	23.7	7.0	18.1	8.9	25.3	3.46	24	5.9
500m(n=31)	23	5.5	17.4	6.7	25.2	2.14	24.8	4.6
1000m(n=31)	24.3	4.6	16	5.1	25	1.7	25.8	3.34
1500m(n=31)	25.1	4.1	14.9	3.9	24.9	1.25	26.5	2.1

4.5   Spatial patterns of key built environment elements in Villach: A Moran's I analysis

According to the spatial autocorrelation analysis (Global Moran's I), Table 4.9 represents the results for green space, construction, transport infrastructure, and sky view reveal significant spatial clustering patterns in Villach. Each land-use category has an observed Moran's index higher than the expected Moran's index under a random distribution, suggesting spatial clustering beyond random chance. The very high z-scores indicate strong clustering effects in each category,

with substantial deviations from the expected mean under randomness. These z-scores and the extremely low p-values (all 0.000000) confirm that the clustering patterns are statistically significant, implying that these land-use features are not randomly distributed across the study area. But the lower General G value also indicates the pattern exists but may not be as tightly clustered.

Table 4.9 presents the results of the spatial autocorrelation analysis (global Moran's I) via ArcGIS Pro (Version 3.0.3, ESRI) for green space, construction, transport infrastructure, and sky view in Villach. Each environmental feature shows a positive Moran's Index significantly, indicating notable spatial clustering. The p-values (all effectively 0) further confirm that these clustering patterns are statistically significant, strongly suggesting that these environmental features are distributed in structured, non-random patterns across Villach. The z-scores are exceptionally high across all categories, which confirms substantial deviations from random spatial patterns. Specifically, construction and green space has the higher Moran's Index, suggesting that built areas are strongly clustered together. While transport infrastructure has the lowest Moran's Index, indicating significant but weaker clustering.

Table 4.9 Results of spatial autocorrelation analysis (global Moran's I)

	Green space	Construction	Transport Infrastructure	Sky view
Moran's Index	0.361165	0.396629	0.189272	0.263286
Expected Index	-0.000293	-0.000293	-0.000293	-0.000293
Variance	0.000017	0.000017	0.000017	0.000017
z-score	88.083489	96.852801	46.197550	64.233325
p-value	0.000000	0.000000	0.000000	0.000000

Figure 4.11 shows the results of cluster and outlier analysis (local Moran's I). For green space, high-high clusters are primarily located on the outskirts of Villach, indicating areas with abundant greenery. Low-low clusters are concentrated in the urban core, suggesting limited green

space in densely built areas. In contrast, construction shows high-high clusters in central Villach, representing densely built-up zones, while low-low clusters are present on the city's periphery, where construction is minimal. Transport infrastructure also forms high-high clusters along main roads and thoroughfares, particularly near major access points to the city, indicating high levels of transport infrastructure in these areas. Sky view shows high-high clusters primarily on the outskirts and low-low clusters in the urban core. This pattern suggests that central areas with tall buildings and dense infrastructure obstruct sky visibility, while open spaces near the periphery offer greater sky exposure.
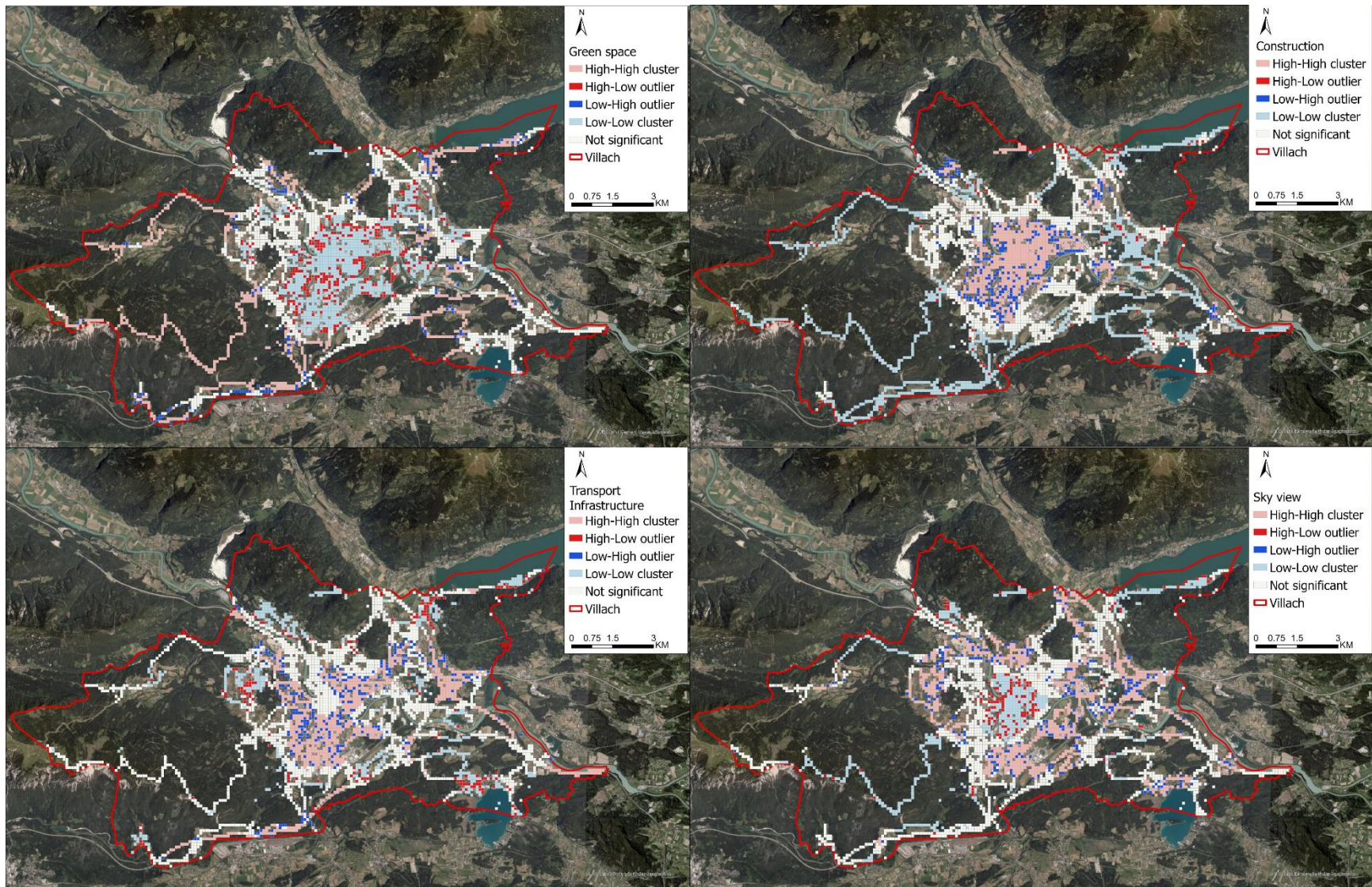
Figure 4.11 Results of cluster and outlier analysis (local Moran's I)

5   Limitation

Regarding the limitations of this study and the direction of future research, first, the model adjustments can be further refined. This study utilizes broader environmental categories to accommodate different models due to the different classification from different datasets. However, this approach sacrifices detail; for example, by grouping roads, sidewalks, and parking under "transport infrastructure," it limits insights into pedestrian and bike lane accessibility that may influence children's active commuting. Additionally, the use of the pre-trained DeepLabv3 model could be enhanced by transitioning to DeepLabv3+, which offers improvements in accuracy and contextual information. Chen et al. (2018) improved DeepLabv3, which employs the spatial pyramid pooling module, with the encoder-decoder structure. Spatial pyramid pooling module emphasized the contextual information at different resolutions, while encoder-decoder structure emphasized object boundaries. The proposed model, DeepLabv3+, contains rich semantic information from the encoder module, while the detailed object boundaries are recovered by the simple yet effective decoder module(Chen et al., 2018). Compared with other mainstream neural network models like PSPNet and SegNet, DeepLabv3+ has shown superior accuracy(Zhang et al., 2023). This suggests that using DeepLabv3+ and training it on locally relevant data could improve classification accuracy in capturing Villach's unique environmental features.

Additionally, the specific analysis of issues in the study area of Villach needs to be strengthened. Villach's mountainous geography presents a unique context that differs from flatland cities, as distant natural elements are often excluded from urban environmental analyses. Current research, including this study, does not consider mountains into the definition of green space or natural factors. The Cityscapes dataset tends to categorize mountains as static objects, treating them as mere background elements in street scenes. There is a lack of exploration into how these

distant landscapes, as seen in GSV imagery, could influence children's health behaviors, similar to proximate green spaces. Future studies should investigate the health impacts of these distant landscapes and how they may enhance children's connection to nature and promote outdoor activities.

6   Future research

Building on the pre-trained model used in this study, future research should refine the image segmentation model to more accurately capture the unique geographic characteristics of Villach, such as its mountainous terrain and water bodies.

This study primarily examines the environment around primary schools but lacks data on children's health behaviors or health status. It provides a foundation for exploring how environmental factors may influence children's health behaviors and for designing healthier urban spaces. However, the scope of this research is limited to primary schools. Future studies could expand the analysis to include various school levels, considering factors like age-related definitions of active commuting, neighborhood safety, and other contextual influences.

An et al.(2017) found the associations between residential neighborhood amenities and children's health behavior were differed by sex, race/ethnicity, parent-rated child health status, and household income level. With the environment measurement and the buffer analysis based on primary school, future research should integrate socio-economic and children's health such as census and physical activity information, to deepen the understanding of environmental disparities and their effects on children's health outcomes, particularly regarding obesity rates.

This study utilizes GSV data by default, which covers 2014 to 2024. Future research can set stricter temporal controls to analyze changes in urban land use over time. For example, by focusing on Villach's development over the past decade, it would be possible to examine whether

green space coverage has increased or decreased. Such analyses could be further linked to children's health outcomes, exploring how environmental changes impact children's health and providing valuable insights into the intersection of urban planning and public health.

7   Conclusion

Google Street View (GSV) imagery provides an objective, quantitative measure of environmental characteristics, though outcomes vary depending on the specific models and datasets used for analysis. This study selects the Deeplabv3 model trained on the ADE20K dataset, which demonstrated effective segmentation performance in Villach. However, model accuracy can differ significantly across categories and locations, for example, the model shows reduced accuracy in detecting construction features in Villach's suburban TPV area. Spatial pyramid pooling module in DeepLabv3 emphasized the contextual information at different resolutions

GSV-based environmental measurement reveals significant differences between Villach's inner city and TPV areas, with the inner city showing less green space and sky view but higher proportions of construction and transport infrastructure. This contrast in land use aligns with the spatial autocorrelation analysis results, which show statistically significant clustering of environmental features across the city. Although Villach, as a whole, generally offers a favorable environment for children's health—characterized by substantial green space and sky view—the areas surrounding primary schools display comparatively lower percentages of green space and sky view. This suggests that, despite the overall positive urban environment, the more densely built surroundings near educational institutions could negatively impact children's access to these beneficial environmental features. However, it is important to note that GSV data coverage is not uniformly available across all regions. Consistent with existing literature, more urbanized areas

have denser GSV coverage, while suburban regions, such as Villach's eastern areas, have limited data.

In sum, by advancing methods for assessing children's environmental exposure, this study contributes to public health research and urban planning, advocating for environments that promote healthy behaviors in children. Additionally, it underscores the need for future studies to refine models for local data and improve classification granularity, particularly in regions with limited GSV coverage or unique geographical contexts, such as Villach's mountainous landscape.

Acknowledgements

References

An, R., Yang, Y., & Li, K. (2017). Residential Neighborhood Amenities and Physical Activity Among U.S. Children with Special Health Care Needs. *Maternal and Child Health Journal*, *21*(5), 1026–1036. https://doi.org/10.1007/s10995-016-2198-3

Barrett, M., Crozier, S., Lewis, D., Godfrey, K., Robinson, S., Cooper, C., Inskip, H., Baird, J., & Vogel, C. (2017). Greater access to healthy food outlets in the home and school environment is associated with better dietary quality in young children. *Public Health Nutrition*, *20*(18), 3316–3325. https://doi.org/10.1017/S1368980017002075

Ben-Joseph, E., Lee, J. S., Cromley, E. K., Laden, F., & Troped, P. J. (2013). Virtual and actual: Relative accuracy of on-site and web-based instruments in auditing the environment for physical activity. *Health & Place*, *19*, 138–150. https://doi.org/10.1016/j.healthplace.2012.11.001

Boeing, G. (2017). New methods for acquiring, constructing, analyzing, and visualizing complex street networks. *Comput Environ Urban Syst*, *65*, 126–139. https://doi.org/10.1016/j.compenvurbsys.2017.05.004

Bosch, L. S. M. M., Wells, J. C. K., Lum, S., & Reid, A. M. (2020). Associations of the objective built environment along the route to school with children's modes of commuting: A multilevel modelling analysis (the SLIC study). *PLOS ONE*, *15*(4), e0231478. https://doi.org/10.1371/journal.pone.0231478

Breda, J., Farrugia Sant'Angelo, V., Duleva, V., Galeone, D., Heinen, M. M., Kelleher, C. C., Menzano, M. T., Musić Milanović, S., Mitchell, L., Pudule, I., Rito, A. I., Shengelia, L., Spinelli, A., Spiroski, I., Yardim, N., Buoncristiano, M., Williams, J., Rakovac, I., & McColl, K. (2021). Mobilizing governments and society to combat obesity: Reflections on how data from the WHO European Childhood Obesity Surveillance Initiative are helping to drive policy progress. *Obesity Reviews*, *22*(S6), e13217. https://doi.org/10.1111/obr.13217

Carver, A., Timperio, A. F., Hesketh, K. D., Ridgers, N. D., Salmon, J. L., & Crawford, D. A. (2011). How is active transport associated with children's and adolescents' physical activity over time? *International Journal of Behavioral Nutrition and Physical Activity*, *8*(1), 126. https://doi.org/10.1186/1479-5868-8-126

CDC. (2022, April 1). *Childhood Overweight & Obesity*. https://www.cdc.gov/obesity/childhood/index.html

Chen, L.-C., Zhu, Y., Papandreou, G., Schroff, F., & Adam, H. (2018). Encoder-Decoder with Atrous Separable Convolution for Semantic Image Segmentation. In V. Ferrari, M. Hebert, C. Sminchisescu, & Y. Weiss (Eds.), *Computer Vision – ECCV 2018* (Vol. 11211, pp. 833–851). Springer International Publishing. https://doi.org/10.1007/978-3-030-01234-2_49

Clarke, P., Ailshire, J., Melendez, R., Bader, M., & Morenoff, J. (2010). Using Google Earth to conduct a neighborhood audit: Reliability of a virtual audit instrument. *Health & Place*, *16*(6), 1224–1229. https://doi.org/10.1016/j.healthplace.2010.08.007

Ding, D., Sallis, J. F., Kerr, J., Lee, S., & Rosenberg, D. E. (2011). Neighborhood Environment and Physical Activity Among Youth. *American Journal of Preventive Medicine*, *41*(4), 442–455. https://doi.org/10.1016/j.amepre.2011.06.036

Durand, C. P., Dunton, G. F., Spruijt-Metz, D., & Pentz, M. A. (2012). Does Community Type Moderate the Relationship between Parent Perceptions of the Neighborhood and Physical Activity in Children? *American Journal of Health Promotion*, *26*(6), 371–380. https://doi.org/10.4278/ajhp.100827-QUAN-290

Feuillet, T., Charreire, H., Roda, C., Ben Rebah, M., Mackenbach, J. D., Compernolle, S., Glonti, K., Bárdos, H., Rutter, H., De Bourdeaudhuij, I., McKee, M., Brug, J., Lakerveld, J., & Oppert, J. -M. (2016). Neighbourhood typology based on virtual audit of environmental obesogenic characteristics. *Obesity Reviews*, *17*(S1), 19–30. https://doi.org/10.1111/obr.12378

Gascon, M., Vrijheid, M., & Nieuwenhuijsen, M. J. (2016). The Built Environment and Child Health: An Overview of Current Evidence. *Current Environmental Health Reports*, *3*(3), 250–257. https://doi.org/10.1007/s40572-016-0094-z

Google. (n.d.). *Google-Contributed Street View Imagery Policy*. https://www.google.com/streetview/policy/#:~:text=Street%20View%20Imagery%20is%20Not,to%20a%20few%20years%20old.

Kang, Y., Zhang, F., Gao, S., Lin, H., & Liu, Y. (2020). A review of urban physical environment sensing using street view imagery in public health studies. *Annals of GIS*, *26*(3), 261–275. https://doi.org/10.1080/19475683.2020.1791954

Kim, J., & Jang, K. M. (2023). An examination of the spatial coverage and temporal variability of Google Street View (GSV) images in small- and medium-sized cities: A people-based approach. *Computers, Environment and Urban Systems*, *102*, 101956. https://doi.org/10.1016/j.compenvurbsys.2023.101956

Larkin, A., & Hystad, P. (2019). Evaluating street view exposure measures of visible green space for health research. *Journal of Exposure Science & Environmental Epidemiology*, *29*(4), 447–456. https://doi.org/10.1038/s41370-018-0017-1

Li, X., Zhang, C., Li, W., Ricard, R., Meng, Q., & Zhang, W. (2015). Assessing street-level urban greenery using Google Street View and a modified green view index. *Urban Forestry & Urban Greening*, *14*(3), 675–685. https://doi.org/10.1016/j.ufug.2015.06.006

Lu, Y., Sarkar, C., & Xiao, Y. (2018). The effect of street-level greenery on walking behavior: Evidence from Hong Kong. *Social Science & Medicine*, *208*, 41–49. https://doi.org/10.1016/j.socscimed.2018.05.022

Malacarne, D., Handakas, E., Robinson, O., Pineda, E., Saez, M., Chatzi, L., & Fecht, D. (2022). The built environment as determinant of childhood obesity: A systematic literature review. *Obesity Reviews*, *23*(S1), e13385. https://doi.org/10.1111/obr.13385

Missbach, B., Pachschwöll, C., Kuchling, D., & König, J. (2017). School food environment: Quality and advertisement frequency of child-oriented packaged products within walking distance of public schools. *Preventive Medicine Reports*.

Ortegon-Sanchez, A., McEachan, R. R. C., Albert, A., Cartwright, C., Christie, N., Dhanani, A., Islam, S., Ucci, M., & Vaughan, L. (2021). Measuring the Built Environment in Studies of Child Health—A Meta-Narrative Review of Associations. *International Journal of Environmental Research and Public Health*, *18*(20), 10741. https://doi.org/10.3390/ijerph182010741

Rzotkiewicz, A., Pearson, A. L., Dougherty, B. V., Shortridge, A., & Wilson, N. (2018). Systematic review of the use of Google Street View in health research: Major themes, strengths, weaknesses and possibilities for future research. *Health & Place*, *52*, 240–246. https://doi.org/10.1016/j.healthplace.2018.07.001

Smith, M., Hosking, J., Woodward, A., Witten, K., MacMillan, A., Field, A., Baas, P., & Mackie, H. (2017). Systematic literature review of built environment effects on physical activity and active transport – an update and new findings on health equity. *International Journal*

of Behavioral Nutrition and Physical Activity, *14*(1), 158. https://doi.org/10.1186/s12966-017-0613-9

Stierman, B., Afful, J., Carroll, M. D., Chen, T.-C., Davy, O., & Fink, S. (2021). National Health and Nutrition Examination Survey 2017–March 2020 Prepandemic Data Files—Development of Files and Prevalence Estimates for Selected Health Outcomes. *National Health Statistics Reports*, *158*.

Ta, N., Li, H., Chai, Y., & Wu, J. (2021). The impact of green space exposure on satisfaction with active travel trips. *Transportation Research Part D: Transport and Environment*, *99*, 103022. https://doi.org/10.1016/j.trd.2021.103022

Wada, K. (n.d.). *Labelme: Image Polygonal Annotation with Python* [Computer software]. https://github.com/wkentaro/labelme

Wang, M., & Vermeulen, F. (2021). Life between buildings from a street view image: What do big data analytics reveal about neighbourhood organisational vitality? *Urban Studies*, *58*(15), 3118–3139. https://doi.org/10.1177/0042098020957198

Wang, R., Helbich, M., Yao, Y., Zhang, J., Liu, P., Yuan, Y., & Liu, Y. (2019). Urban greenery and mental wellbeing in adults: Cross-sectional mediation analyses on multiple pathways across different greenery measures. *Environmental Research*, *176*, 108535. https://doi.org/10.1016/j.envres.2019.108535

World Health Organization. (n.d.). *Children's environmental health*. Retrieved October 1, 2023, from https://www.who.int/health-topics/children-environmental-health#tab=tab_2

Xia, Y., Yabuki, N., & Fukuda, T. (2021). Sky view factor estimation from street view images based on semantic segmentation. *Urban Climate*, *40*, 100999. https://doi.org/10.1016/j.uclim.2021.100999

Yu, H., Chen, C., Du, X., Li, Y., Rashwan, A., Hou, L., Jin, P., Yang, F., Liu, F., & Li, J. (2020). *TensorFlow Model Garden* [Computer software]. https://github.com/tensorflow/models

Zhang, L., Wang, L., Wu, J., Li, P., Dong, J., & Wang, T. (2023). Decoding urban green spaces: Deep learning and google street view measure greening structures. *Urban Forestry & Urban Greening*, *87*, 128028. https://doi.org/10.1016/j.ufug.2023.128028